AJNR Am J Neuroradiol 24:1849–1856, October 2003

Differential Aging of the Human Striatum: Longitudinal Evidence

Naftali Raz, Karen M. Rodrigue, Kristen M. Kennedy, Denise Head, Faith Gunning-Dixon, and James D. Acker

BACKGROUND AND PURPOSE: **Information about age-related changes in the striatum comes almost exclusively from cross-sectional studies. We examined age-related differences and longitudinal changes in the volume of the striatal nuclei, compared longitudinal measures of changes with their cross-sectional estimates, and addressed the question of differential aging of the basal ganglia.**

METHODS: **We measured the volumes of the caudate nucleus (head), the putamen, and the globus pallidus on MR images of 53 healthy adults whose ages at baseline ranged between 20 and 77 years. The measurements were conducted twice, 5 years apart.**

RESULTS: **On both measurement occasions, the volume of the neostriatal nuclei (caudate and putamen) but not of the globus pallidus correlated negatively with age. However, longitudinal comparison revealed significant declines in the neostriatal volumes and smaller (but statistically significant) shrinkage of the paleostriatum. In 5 years, the striatal components (caudate, putamen, and globus pallidus) shrunk by 1.21, 0.85, and 0.55 standard deviation units, respectively. The average annual shrinkage rate was 0.83% in the caudate nucleus, 0.73% in the putamen, and 0.51% in the globus pallidus.**

CONCLUSION: **Although cross-sectional estimates suggested preservation of some striatal nuclei, longitudinal shrinkage of the whole striatum was evident even in a selected group of healthy adults. Moreover, the magnitude of observed longitudinal change was greater than predicted from cross-sectional studies.**

The striatal nuclei—caudate, putamen, and globus pallidus—play a critical role in the planning, execution, and control of movement (1) and in acquisition of motor sequences (2). Cross-sectional studies of humans (3) and other primates (4) indicate that old age is associated with reduced volumes of the neostriatum (caudate nucleus and putamen), whereas age differences in the volume of paleostriatum (globus pallidus) are significantly smaller (5, 6). The extent of age-related differences in the volume of some striatal nuclei may vary between the sexes (6), and shrinkage of the putamen may mediate age deficits in skill acquisition (7).

The estimates of age-related changes in striatal volume have been almost exclusively derived from cross-sectional studies (3). The main limitation of the cross-sectional design is its sensitivity to individual differences and cohort effects: the former may result in underestimation of true age-related change, whereas the latter may exaggerate it. Both of these threats to validity are controlled in the longitudinal design. To date, four longitudinal MR imaging studies have incidentally addressed some aspects of age-related changes in the adult human striatum (8–11). None of those studies was designed to examine age-related change, and all were limited to small samples (n = 10–20) of young healthy control subjects who were compared with patients who had first episodes of schizophrenia. Also, the scope of anatomic measures conducted in those investigations was limited. Three studies were restricted to assessment of the caudate nucleus (8–10); in the fourth, a short (1-year) follow-up of all three striatal nuclei was conducted (11). Significant declines in the caudate volume were observed in two of the longitudinal studies. An 18-month follow-up (8) indicated a significant shrinkage of the caudate (annualized percent change [APC] = 1.07%), whereas a 5-year follow-up (10) revealed an even greater decline of the caudate volume in healthy subjects (APC = 1.86%). In the other two studies (9,

Received February 26, 2003; accepted after revision May 13.

From the Institute of Gerontology and Department of Psychology (N.R., K.M.R., K.M.K.), Wayne State University, Detroit MI; Department of Psychology (D.H.), Washington University, St. Louis, MO; Department of Psychology (F.G.-D.), Long Island Jewish Medical Center, Glen Oaks, NY; Diagnostic Imaging Center (J.D.A.), Baptist Memorial Hospital-East, Memphis, TN

Address correspondence to Naftali Raz, PhD, Institute of Gerontology, 87 E. Ferry Street, Detroit, MI 48202.

11), no significant changes in the volume of any of the examined basal ganglia were observed after 1–5-year follow-up examinations. Study characteristics, such as restricted age ranges and small samples, limit the impact of these findings on our understanding of brain aging. None of the studies addressed the question of sex differences, and none compared the estimates of age-related shrinkage derived from cross-sectional and longitudinal studies. In addition, in some of the studies, the follow-up measures were constrained by the MR imaging technology available at the initial examination. For instance, in one study (9), only two to three thick (5-mm) axial sections were used to estimate the caudate volume.

Measurement of the basal ganglia in adults presents a challenge. Striatum tends to accumulate more iron than most of the other brain regions, with the iron concentration being especially high in the globus pallidus (12, 13). Thus, MR imaging–based measures of the pallidal volume could have been insensitive to age-related shrinkage as long as calcium and iron deposits were included in the volume of the nucleus. Also, of all the basal ganglia, the globus pallidus contains the greatest number of dilated perivascular spaces and cysts, which become more prevalent with age and may contribute to the volume of the region of interest (ROI) but not to its functional integrity (14). Volumetric investigations of the basal ganglia have rarely assessed a potentially confounding effect of inorganic inclusions (eg, calcification or iron deposits), nonneural tissue (eg, gliosis), or fluid-filled (Virchow-Robin) spaces on the measured volume. Thus, assessment of the contribution of nonneural inclusions to the volume of the globus pallidus may help to understand the differential effects of age on its volume.

The main objective of this study was to gauge the change in regional striatal volumes while controlling for individual differences. We hypothesized that the longitudinal examination would reveal a clearer pattern of age-related preservation and decline along the lines suggested by the cross-sectional studies. Specifically, on the basis of the cross-sectional literature, we expected to observe moderate shrinkage of the caudate and the putamen but not of the pallidum.

Methods

Sample

Initially, subjects were recruited for multiple cross-sectional studies of healthy-aging brain and cognition by advertising in local media in a major metropolitan area in the United States and on an urban university campus. The participants signed an informed consent form approved both by the university's Committee for Protection of Human Subjects in Research and by the hospital's Patients Participation Committee. To screen the potential participants for health problems that might adversely affect brain morphology and cognitive performance, we used a mail-in 66-item questionnaire augmented by telephone and personal interviews. Persons who reported a history of cardiovascular, neurologic, or psychiatric conditions; head trauma with loss of consciousness for more than 5 minutes; thyroid problems; diabetes; treatment for drug and/or alcohol abuse; or a habit of taking more than three alcoholic drinks per day were excluded from the study, as were persons who reported taking antiseizure medication, anxiolytics, antidepressants, or recreational drugs. Persons who had or suspected they could have claustrophobia were advised against participation in the study. All subjects were screened for dementia and depression with a modified Blessed Information-Memory-Concentration Test (15) (cutoff = 30) and Geriatric Depression Questionnaire (16) (cutoff = 15). All participants were consistent right-handers (score above 75% on the Edinburgh Handedness Questionnaire [17]).

An experienced neuroradiologist (JDA) examined the MR images for signs of space-occupying lesions and signs of significant cerebrovascular disease. Specifically, we excluded all participants with MR imaging evidence of infarct, focal parenchymal loss that may result from infarct, coalescing and large patchy areas of white matter hyperintensity on T2-weighted images, and occluded vessels. We accepted few focal white mater hyperintensities on T2-weighted images without associated hypointensities on T1-weighted images.

Subjects who participated in previous cross-sectional studies were contacted by mail and telephone. We attempted to locate all 284 participants who would be eligible for follow-up after a 5-year delay, and 188 (66%) responded to invitation. Of those, 126 (67%) agreed to participate in the study. Less than half of the respondents passed the health screening criteria and had valid MR imaging data. That sample (n = 53, 19% of the eligible cohort) consisted of 23 men and 30 women. The mean duration of the follow-up delay was 5.24 ± 0.27 (SD) years, with a range of 4.92–6.00 years. There was a small (< 2 months) but a significantly reliable difference between men and women in the duration of follow-up delay (5.33 years for men vs 5.17 years for women, $t = 2.07$, $P < .05$). The age of the participants at the second testing ranged between 26 and 82 years, with a mean age at follow-up of 57.06 ± 15.02 years (53.00 for men and 60.17 for women; $t = 1.69$, not significant [NS]). The mean years of education in this sample was 16.15 ± 2.58 years, equivalent to a typical college education; men and women did not differ in duration of formal education: 15.63 years for women versus 16.83 years for men ($t = 1.68$, NS). Most Mini Mental State Examination (MMSE) (18) scores at the time of second imaging were substantially higher than the cutoff of 26 (mean 28.98 ± 1.02) and were unrelated to age ($r = -0.03$, NS) or sex ($t = 0.48$, NS). Eleven participants (four men and seven women; mean age, 69.18 ± 12.34 years) with diagnosed and medically controlled hypertension were also included in the sample. They were older than the remainder of the sample (60.81 vs 47.95 years, $t = 3.09$, $P < .01$), but had the same years of formal education and equivalent MMSE scores (both $t < 1.0$, NS).

MR Imaging Protocol

All imaging for the base-line measurements was performed with a 1.5-T system (Signa; GE Medical Systems, Milwaukee, WI). At the beginning of each session, a 40-second seven-section T1-weighted sagittal localizer series was acquired with 400/16 (TR/TE) and a 5-mm section thickness. After positioning the sections, two sequences were acquired. To screen subjects with cerebrovascular disease, a fast spin-echo, double-echo sequence of T2- and proton-density–weighted axial images was acquired, with 3300/90, 18/1 (TR/TE effective/excitation), 5-mm section thickness, and 2.5-mm intersection gap. Volumes were measured on the images acquired with a T1-weighted 3D spoiled gradient-recalled sequence with 124 contiguous axial sections, 24/5/1 (TR/TE/excitation), 22-cm field of view, acquisition matrix of 256 × 192, 1.3-mm section thickness, and flip angle of 30°.

All follow-up imaging was performed with a 1.5-T system (Signa; GE Medical Systems) installed in the same hospital. However, whereas only one magnet was used for the initial examination (time 1), an additional magnet of the same make and model was used for retesting (time 2) of four subjects. All

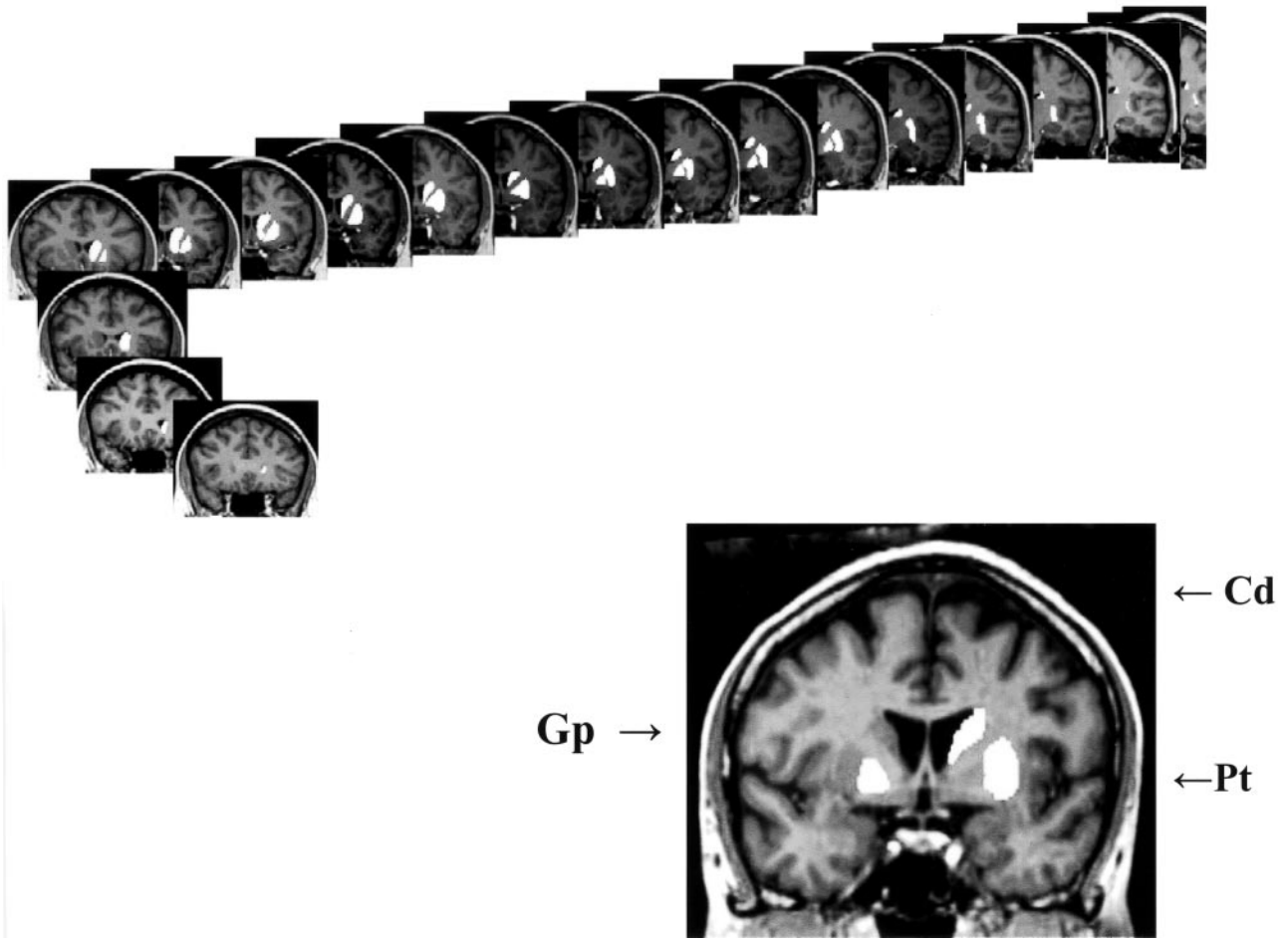

FIG 1. An example of demarcation and tracing of three striatal regions of interest (caudate, putamen and globus pallidus) on a series of coronal images.

subjects were imaged with identical pulse sequences on both measurement occasions, and the MR systems were routinely calibrated by using the same standard GE phantom. The images acquired on both occasions (time 1 and time 2) were coded, and the order of tracing was randomized within each subject by a person other than the operators who traced the ROIs. The operators (KMR, KMK, DH) were blind to the chronology of the specific images, the demographic characteristics of the participants, and the magnet on which the image was acquired.

Volumetric Image Analysis

The data were reformatted to correct for undesirable effects of head tilt, pitch, and rotation with BrainImage 2.3.3 software available online at http://www.stanford.edu/group/cap/research/neuroimaging/imageanalysis. The realignment process, described in greater detail elsewhere (19), consisted of the following steps. First, the axial plane was tilted so it passed through the anterior and posterior commissures (incorporating the anterior commissure–posterior commissure line). Second, the axial plane was rotated to pass through the orbits in such a way that the axial cross section of the orbits on the right and left sides of the head was of equal diameter. Third, the sagittal plane was moved to pass along the straight line drawn through the extreme anterior and posterior points of the interhemispheric fissure. Finally, the coronal plane was drawn perpendicular to the axial and sagittal planes as defined. The reformations were partitioned into 1.5-mm contiguous coronal sections.

Region Demarcation and Tracing Rules

The ROIs were measured with National Institutes of Health (NIH) Image software (version 1.60, available at http://rsb.info.nih.gov/nih-image/), and the volumes were computed by multiplying the sum of the areas by section thickness and the scaling factor derived from calibration measurements of the phantom images. A calibration factor was derived for each magnet involved in the study. The ROIs were defined and traced according to the rules outlined below. The measurements were calibrated for each image by using MR system–specific phantom images. All anatomic landmarks, sulci, and regional borders were ascertained by using standard atlases (20, 21). An example of a traced series of the striatal ROIs is presented in Figure 1.

Intracranial Volume (ICV).—The intracranial volume was estimated from the coronal sections. The operator traced intracranial volume on every eighth section (a total of 11–12 sections) between the first section following the orbits and the last section on which brain tissue was visible. Tracing began at the right side of the head and proceeded clockwise following the inner table of the skull until the homologous mark was reached on the left side of the head, at which point the tracing contour was allowed to close automatically by drawing a straight line back to the origin.

Caudate Nucleus.—The volume of the head and body of the caudate nucleus was estimated from 15–20 coronal sections. The most rostral section was the one on which the caudate first appeared, usually lateral to the lateral ventricles. The caudate

was traced on ever other section until it was no longer visible. The lateral ventricle defined the medial boundary of the caudate, the internal capsule served as its lateral border, and the white matter demarcated its dorsal limit. On the rostral sections, the stria terminalis constituted the ventral boundary. On more anterior sections of the caudate nucleus, the septal nucleus served as the ventral border. The transition between the caudate nucleus and the septal nucleus was often difficult to determine, so the ventral border was defined as a line drawn from the most ventral part of the internal capsule to the most ventral part of the lateral ventricle.

Putamen.—The volume of the putamen was estimated from 15–20 coronal sections. We began tracing on the most rostral section on which the putamen was visible and continued to the most caudal section on which it could be detected. The external capsule demarcated the putamen laterally throughout the ROI. The dorsal boundary of the putamen was white matter. The internal capsule delineated the medial border until the anterior commissure was reached. At this point, the globus pallidus became the medial border of the putamen. The temporal stem, optic radiations, amygdala, temporal horn, and anterior commissure served as the ventral boundary of the putamen. The putamen was measured on every other section until it was no longer visible.

Globus Pallidus.—Because of poor resolution on the most rostral regions, globus pallidus was measured on every section from the anterior commissure to the mammillary bodies (a total of six to eight sections). In some cases, globus pallidus may be difficult to separate from the putamen on the sections preceding the anterior commissure. This addition of volume to the putamen was probably negligible, whereas addition of putamen (a much larger structure) volume to globus pallidus would have introduced a substantial bias. Thus, in questionable cases, we erred in the direction of the putamen. The internal capsule served as the medial border of the globus pallidus, whereas the lateral border was marked by the putamen. On the rostral sections, the anterior commissure marked the ventral border of the globus pallidus, and on the caudal sections, that role was played by preoptic and olfactory areas.

Reliability of manually traced ROI volumes was assessed by using a conservative intraclass correlation (ICC-2) formula that presumes random selection of raters (22). Median values of ICC-2 for all pairs of three operators were 0.95 for caudate nucleus and 0.96 for putamen and globus pallidus. No pair of operators had ICC-2 lower than 0.90 for globus pallidus, 0.91 for caudate nucleus, or 0.92 for putamen.

Evaluation of Nonneural Inclusions in the Globus Pallidus

To evaluate the potential influence of nonneural inclusions in the globus pallidus on its volume and apparent annual shrinkage, we performed a semiquantitative assessment of the total burden of hypointense areas in that ROI. The imaging sequence used in this study was designed to optimize the anatomic measures and did not permit fine-grain analysis of the etiologic distinction among hypointense areas in the globus pallidus. However, all of the major nonneural inclusions (calcification, ferritin deposits, and expanded perivascular spaces) are presumed to detract from functionality of the neural circuitry. Thus, we designed a rating scale (Appendix) that assigned a severity rating from 0 to 4 to the globus pallidus hypointensities on all sections on which it was observed. Reliability of the scale for two raters was an ICC-2 of 0.96.

Results

The 5-year change in the volume of striatal nuclei was evaluated in a mixed general linear model, in which the adjusted regional volume was the dependent variable; three regions of interest (caudate, putamen, and globus pallidus), hemisphere (left vs right), and measurement occasion (baseline vs 5-year follow-up) were categorical within-subject factors; age at baseline (recentered at the sample mean) was a continuous independent variable; and sex was a categorical between-subjects variable. Before the analyses, all brain volumes were adjusted by using the covariance approach. The adjusted volumes were computed from a linear equation: $\text{volume}_{\text{adj}i} = \text{volume}_{\text{raw}i} - b(\text{ICV}_i - \text{ICV})$ for each subject i, where $\text{volume}_{\text{adj}i}$ is adjusted volume of a given ROI, $\text{volume}_{\text{raw}i}$ is raw volume of that ROI, b is slope of ROI volume regression on ICV, and mean ICV is a sample mean of the intracranial volume. In each case, the homogeneity of regression slopes (absence of sex × ICV interaction) was checked to allow the use of a common slope for both sexes. The intracranial volume was not correlated with age among men and women (r range = −0.07 to 0.11, all NS), nor did it change during the 5-year follow-up ($t < 1.0$).

The results of the mixed linear model analysis revealed a clear overall decline in striatal volume during the 5-year period: main effect of time, $F_{1,49} = 77.52$, $P < .001$. However, a significant time × ROI interaction ($F_{2,98} = 17.80$, $P < .001$) indicated that during the period of 5 years not all striatal regions shrunk to the same extent. The analysis of simple effects showed that the neostriatal nuclei evidenced substantial shrinkage as gauged by the effect size measure: $d = 1.21$ for the caudate and $d = 0.85$ for the putamen (both $P < .001$). In contrast, the globus pallidus showed a substantially smaller though statistically significant reduction in volume: $d = 0.55$ ($P < .05$). The APC was 0.83% for the caudate, 0.73% for the putamen, and 0.51% for the globus pallidus. The change in volume of the caudate was greater than the change in volume of the globus pallidus ($t = 2.35$, $P < .05$) but equivalent to that of the putamen ($t < 1.0$), which, in turn, did not differ from that of the globus pallidus APC ($t = 1.45$, NS).

As indicated by nonsignificant time × hemisphere ($F < 1.0$, NS), time × age ($F = 1.71$, NS), and time × sex ($F < 1.0$) interactions, shrinkage was equivalent in both hemispheres for men and women across the age range. In all three ROIs and on both measurement occasions, the right hemisphere was larger than the left: main effect of hemisphere, $F_{1,49} = 15.78$, $P < .001$. The asymmetry at time 1 and time 2 was 0.94% and 1.27%, respectively, for the caudate; 0.57% and 1.46% for the putamen; and 3.21% and 3.45% for the globus pallidus. Shrinkage of the caudate was associated with volume reduction of the putamen ($r = 0.33$, $P < .05$) and of the globus pallidus ($r = 0.27$, $P < .05$).

Cross-sectional age-related differences were observed at both measurement occasions (main effect of age, $F_{1,49} = 12.96$, $P < .001$), but not for all ROIs (ROI × age interaction, $F_{2,98} = 10.78$, $P < .001$). The effect was uniform across the hemispheres, as indicated by a nonsignificant ROI × age × hemisphere interaction ($F < 1.0$). The ROI × age interaction reflected the difference in regression slopes of vol-

TABLE Cross-Sectional Age-Related Differences in Striatal Volumes Measured Five Years Apart

	Raw Volume						Regression of ICV-Adjusted Volume on Age						
	Time 1			Time 2			Time 1			Time 2			
Nucleus	Mean	SD	CV	Mean	SD	CV	Slope	SE	r_{age}	Slope	SE	r_{age}	r_{12}
Caudate	9.42	1.14	0.12	9.00	1.09	0.12	−.031	.010	−.41	−.034	.009	−.47	.95
Putamen	10.41	0.98	0.09	10.01	1.02	0.10	−.030	.008	−.46	−.033	.008	−.49	.89
Globus Pallidus	2.16	0.27	0.12	2.10	0.27	0.13	.004	.002	.22	.004	.002	.21	.93

Note.—CV (coefficient of variation) is a ratio of standard deviation (SD) to the mean. The regression slopes are unstandardized regression coefficients measured in cc/year. SE is standard error of slope. All coefficients for the caudate nucleus and putamen are significantly different from zero, whereas those for the globus pallidus are not. The differences in slopes between the neostriatum (caudate and putamen) and paleostriatum are statistically significant ($p < .05$). Correlations are Pearson product moment coefficients. All correlations $r > .23$ are significantly different from zero.

ume on age across the nuclei as presented in Table 1 and Figure 2.

Neostriatal volumes were significantly associated with age on both testing occasions, whereas the volume of the globus pallidus was not. The differences between the magnitude of age effects on the caudate and the putamen versus globus pallidus were significant: Steiger (23) $Z^* = 3.49$, $P < .001$ for the closest pair of correlations. There was no overall effect of sex on adjusted regional volumes ($F < 1.0$, NS), although a nonsignificant trend for sex × age interaction was noted: $F_{1,49} = 2.92$, $P < .10$. None of the examined volume-age trends showed a significant nonlinear component (all $F < 1.0$). Age-related shrinkage rate was estimated from cross-sectional data by means of regression equations that were used to compute the predicted volumes of the striatal nuclei at ages 20 and 80 years. The difference was divided by the volume predicted at age 20 years and by 60 (years in the estimated span). The produced estimates (at each

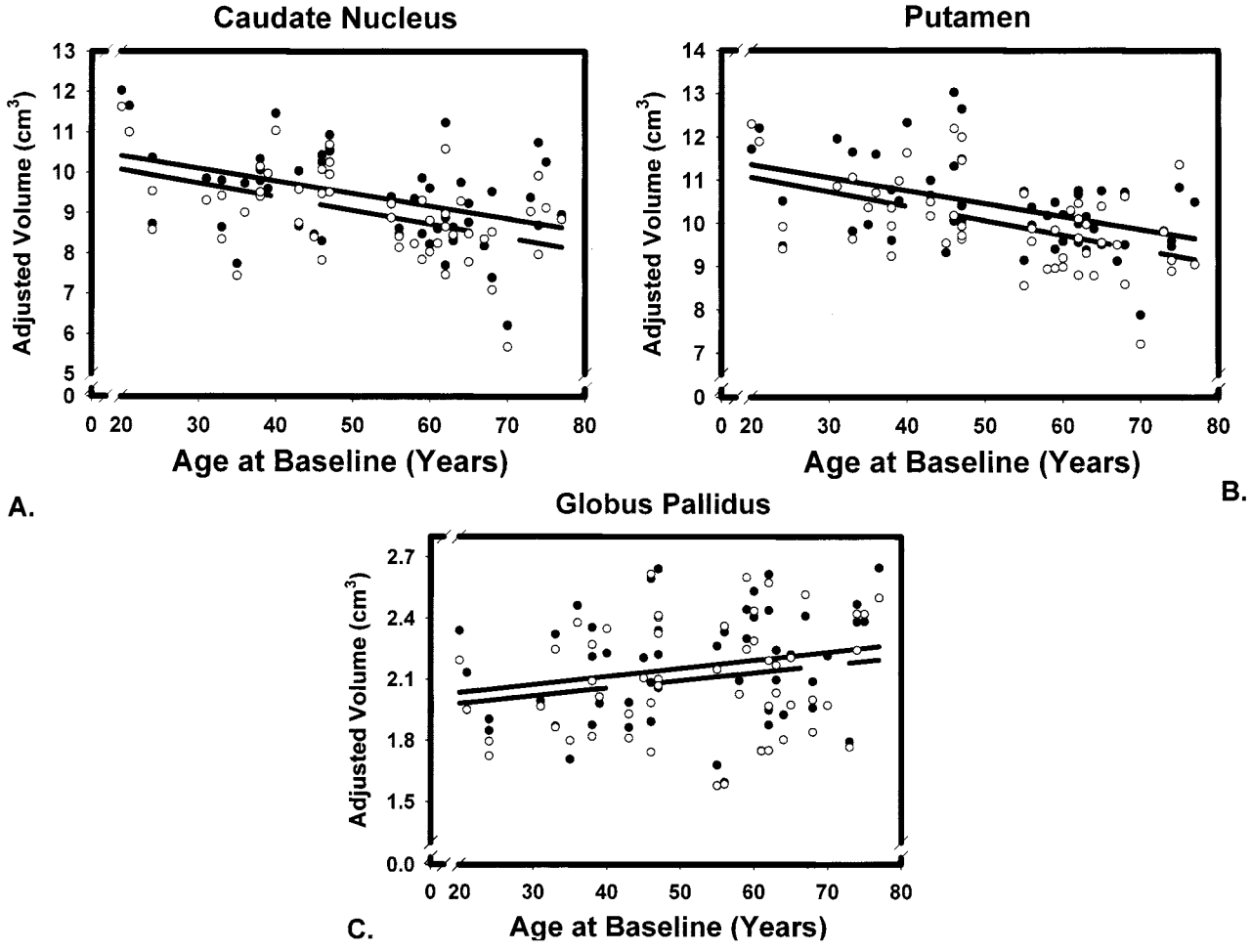

FIG 2. Scatter plots for two volumetric measures of three striatal regions of interest taken on 53 subjects 5 years apart. The lines indicate linear regression of adjusted volumes on age at time 1 (*solid line*) and time 2 (*broken line*). Observations at time 1 are represented by *solid circles*, and observations at time 2 by *empty circles*. Regional volumes are adjusted for the intracranial volume.

measurement occasion) were 0.33% and 0.30% per annum for the caudate and 0.26% and 0.29% for the putamen. There was no estimated decline in the pallidal volume.

The observed age effects could have been confounded by the unequal prevalence of hypertension across the sampled age range. To ascertain that was not the case, we reanalyzed the data without the participants who had hypertension and without those in whom hypertension was diagnosed during the 5 years of follow-up. The observed pattern of effects did not change. When hypertensive participants were compared with the normotensive ones, no differences in annual percentage of shrinkage in any of the three ROIs were observed (all $t < 1.20$, NS).

Finally, we assessed the potentially confounding influence of nonneural inclusions (calcification, iron deposits, and expanded Virchow-Robin spaces) on the measured volume and annual volume change of the globus pallidus. Hypointense areas were found in the globus pallidus on 21 T1-weighted images. Subjects whose globus pallidus included hypointense areas on T1-weighted images were older (60.81 vs 47.95 years, $t = 3.09$, $P < .01$) than those who showed no such hypointensities, and severity of nonfunctional inclusion correlated with age (Spearman $\rho = 0.54$, $P < .001$). However, no correlations were observed between the burden of inclusions and the annualized shrinkage (Spearman $\rho = -0.10$ and $\rho = -0.07$ for time 1 and time 2, respectively, both NS) or burden of inclusions and the adjusted volume of the pallidum (Spearman $\rho = 0.10$ and $\rho = 0.11$ at time 1 and time 2, respectively, both NS). The ratings of pallidal hypointensities at time 1 and time 2 were very highly correlated (Spearman $\rho = 0.99$, $P < .001$). No significant longitudinal change was observed in the hypointensities rating, although in three subjects in their 60s (one woman and two men), an increase of the nonneural burden in the globus pallidus was registered.

Discussion

At the inception of the study, our expectation (based on the extant cross-sectional literature) was that the caudate nucleus and the putamen would evidence moderate shrinkage, but that the pallidum would remain stable. Indeed, we replicated these findings in this sample on both measurement occasions, with correlations of the caudate and putamen volumes with age being very close to the median values of $r = -0.47$ and -0.44 computed across the published studies (3). By contrast, although the results of the longitudinal study revealed age-related shrinkage of the caudate and the putamen as predicted by cross-sectional studies, the rates of decline were substantially larger than suggested by the regression-based estimates (3). In addition, contrary to expectation, we found a significant decline in gross volume of the globus pallidus. Although the shrinkage of the pallidum was smaller than that of the caudate, it still was significantly greater than zero.

The annual shrinkage rate of the caudate was greater than that reported in two small and age-restricted samples (9, 11), comparable to the rate observed in another small sample (8), and somewhat smaller than that in a fourth study (10). We believe that the estimates of longitudinal change reported here and obtained in a larger sample covering a broad age range are more reflective of the true population values. The observed pattern of differential aging cannot be explained away as an artifact of differential reliability, variability, or stability of measures, as reliability (intraclass correlations), stability (time 1–time 2 correlations), and variability (coefficient of variation) were equivalent across all measured structures. Notably, age-related differences were not confined to older adults, but appeared to be linear and uniform across the examined age range. Also, a steady life-span decline in the neostriatal volume was not confined to the adult age span, but is consistent with reported age-related differences in younger adults (24) and even in adolescents (25).

The mechanisms of age-related shrinkage of the basal ganglia are unknown. The mammalian striatum is a cytoarchitectonically diverse region, and its α-aminobutyric acid (GABA)-ergic components are differentially vulnerable to hypoxia, ischemia, and hypoglycemia (26). Transaxonal degeneration of the neurons receiving dopaminergic projections from the substantia nigra is another possible contributor to striatal shrinkage. Notably, the observed rates of shrinkage are comparable to the estimates for age-related loss of striatal dopaminergic indicators (27–29). Although such coincidence cannot be taken as a proof of the association, its absence would have made the notion of dopaminergic mechanisms behind the observed phenomena rather unlikely.

Regardless of the underlying mechanisms, the findings presented here have several implications for future research on brain aging. First, they show that brain shrinkage is a real phenomenon and not an artifact of cohort effects and secular trends. Second, they reinforce the admonition to functional imaging researchers to take into account age-related structural changes that are more substantial than cross-sectional studies led us to believe. To date, we know of only one study (30) of age-related differences in dopamine binding in primate striatum in which correction for age-related shrinkage has been applied. Third, our findings suggest that, as previously hypothesized (31), the caudate nucleus should be considered a highly suitable candidate for explaining age-related changes in behavior and cognition. From a practical perspective, observing decline in the caudate volume, which judging by the magnitude of the effect should be discernible to the naked eye, should not necessarily lead to a suspicion of abnormality.

Methodological Limitations

Because the studies were conducted with the intention to study healthy aging, the reported results were observed in a selected, nonrepresentative sample. The participants were well-educated and highly mo-

tivated healthy volunteers who represented less than a quarter of the original highly selective sample. Individuals with common age-related diseases were not included in the analysis. Therefore, the observed age-related shrinkage of the basal ganglia probably reflects the best-case scenario of successful aging rather than a typical course of senescence.

As in any other in vivo study of the aging brain, image analysis methods could have influenced the results. Measuring age differences in brain volumes faces threats to its validity because age is associated with changes in T1 relaxation time (32) that determines image contrast. The age-T1 relationship is curvilinear (quadratic), and it predicts progressively smaller decrements of T1 with age. The local minimum of T1 is reached at different ages in different brain structures. The cortex shows decline into the 60s, whereas T1 shortening in the putamen levels off at the end of the 3rd decade. In older brains, age-related shortening of gray matter T1 time constant may cause gray matter pixels to appear more similar to their white matter neighbors than they do in younger brains. This confound may cause the structures with earlier expected minima of T1 to appear more age-stable than those in which T1 continues to decline until later age. The impact of this potential confound is unclear and merits further investigation. In any case, the analysis of hypointensities in the globus pallidus on T1-weighted images reveals that regardless of the nature and pathophysiologic origin of the nonneuronal components, lack of volumetric shrinkage of the paleostriatum is probably not an artifact of their inclusion in the ROI volume.

Definitions of ROIs were aimed at maximizing both anatomic validity and reliability of measurement, with results reflecting a compromise between those demands. Thus, as in previous volumetric studies, the terms caudate, globus pallidus, and putamen refer to ROIs that cover less than the anatomic totality of the actual nuclei. Considerations of reliability led to some minor truncation of the volumes to measurable regions and precluded, for example, separate measures of the internal and external nuclei of the globus pallidus. Nonetheless, a good correspondence between the volumes of the neostriatal nuclei measured in this study (Table 1) and the literature (33) supports the validity of the measures.

Finally, a question that arises in any longitudinal study is whether the results are affected by alteration of the measurement instruments. In this study, although the same sequence, field strength, and magnets were used at baseline and follow-up, the MR imaging systems differed and some inevitable upgrades of software occurred in that period. Changes in hardware and software upgrades may alter gray-white contrast and thus bias the measurements. However, all measures were calibrated by using magnet-specific phantoms, and regional volumes were corrected for the intracranial volume, which was not affected by the transition. Thus, although even minor changes in the instruments may introduce noise in the measurements, systematic MR system–related bias in longitudinal measures is very unlikely. A recent study suggests that in practical terms, even significant changes in MR system hardware do not contribute significantly to longitudinal changes in brain volume (34). Thus, relatively minor upgrades in the MR systems used in this study can hardly be considered a threat to the validity of the findings.

Conclusion

The results reported here establish that the human striatum shrinks with age and that the rate of shrinkage varies among the striatal components. The actual longitudinal change appears greater than predicted from cross-sectional estimates. Unlike robust age differences and longitudinal changes observed in the caudate and putamen, the reduced effects of age on the globus pallidus may require further, more definitive studies.

Appendix

The following guidelines were used in ranking the nonneural inclusions.

Absent (0).

Minimal (1): Very small (< 7 pixels) hypointense areas are present on up to 25% of globus pallidus sections.

Mild (2): Very small (< 7 pixels) hypointense areas are present on up to 50% of globus pallidus sections.

Moderate (3): Hypointense areas are present on at least 50% of globus pallidus sections. Medium-sized (7–15 pixels) hypointense areas are apparent on at least one section. Many of the sections may have several small (< 7 pixels each) hypointense areas, either concentrated or dispersed.

Severe (4): Hypointense areas are present on at least 75% of globus pallidus sections that are traced. At least one large (> 15 pixels) hypointense area is present on at least one section. In addition, small and medium-sized hypointense areas may be distributed throughout the globus pallidus.

References

1. Alheid GE, Switzer RC III, Heimer L. Basal ganglia. In: Paxinos G, ed. *The Human Nervous System.* San Diego: Academic Press, 1990: 438–532
2. Nakamura T, Ghilardi MF, Mentis M, et al. **Functional networks in motor sequence learning: abnormal topographies in Parkinson's disease.** *Hum Brain Mapp* 2001;12:42–60
3. Raz N. **Aging of the brain and its impact on cognitive performance: integration of structural and functional findings.** In: Craik FIM, Salthouse TA, eds. *Handbook of Aging and Cognition*–II. Mahwah, NJ: Erlbaum, 2000:1–90
4. Matochik JA, Chefer SI, Lane MA, et al. **Age-related decline in striatal volume in monkeys as measured by magnetic resonance imaging.** *Neurobiol Aging* 2000;21:591–598
5. Hokama H, Shenton ME, Nestor PG, et al. **Caudate, putamen, and globus pallidus volume in schizophrenia: a quantitative MRI study.** *Psychiatry Res* 1995;61:209–229
6. Raz N, Williamson A, Gunning-Dixon F, Head D, Acker JD. **Neuroanatomical and cognitive correlates of adult age differences in acquisition of a perceptual-motor skill.** *Microscopy Res Tech* 2000;51:85–93
7. Gunning-Dixon FM, Head DP, McQuain JM, Acker JD, Raz N.

Differential aging of the human striatum: a prospective MR study. *AJNR Am J Neuroradiol* 1998;1501–1507
8. Chakos MH, Lieberman JA, Bilder RM, et al. **Increase in caudate nuclei volumes of first-episode schizophrenic patients taking antipsychotic drugs.** *Am J Psychiatry* 1994;151:1430–1436
9. DeLisi LE, Sakuma M, Tew W, Kushner M, Hoff AL, Grimson R. **Schizophrenia as a chronic active brain process: a study of progressive brain structural change subsequent to the onset of schizophrenia.** *Psychiatry Res* 1997;74:129–140
10. Tauscher-Wisniewski S, Tauscher J, Logan J, Christensen BK, Mikulis DJ, Zipursky RB. **Caudate volume changes in first episode psychosis parallel the effects of normal aging: a 5-year follow-up study.** *Schizophr Res* 2002;58:185–188
11. Lang DJ, Kopala LC, Vandorpe RA, et al. **An MRI study of basal ganglia volumes in first-episode schizophrenia patients treated with risperidone.** *Am J Psychiatry* 2001;158:625–631
12. Hallgren B, Sourander P. **The effect of age on the non-haemin iron in the human brain.** *J Neurochem* 1958;3:41–51
13. Barzokis G, Sultzer D, Cummings J, et al. **In vivo evaluation of brain iron in Alzheimer disease using magnetic resonance imaging.** *Arch Gen Psychiatry* 2000;57:47–53
14. Braffman BH, Trojanowski JQ, Atlas SW. The aging brain and neurodegenerative disorders. In: Atlas SW, ed. *Magnetic Resonance Imaging of the Brain and Spine*. New York: Raven, 1991: 567–624
15. Blessed G, Tomlinson BE, Roth M. **The association between quantitative measures of dementia and senile change in the cerebral grey matter of elderly subjects.** *Brit J Psychiat* 1968;114:797–811
16. Radloff LS. **The CES-D scale: a self-report depression scale for research in the general population.** *Appl Psych Measure* 1977;1:385–401
17. Oldfield RC. **The assessment and analysis of handedness.** *Neuropsychologia* 1971;9:97–113
18. Folstein MF, Folstein SE, McHugh PR. **"Mini-mental state". A practical method for grading the cognitive state of patients for the clinician.** *J Psychiatry Res* 1975;12:189–198
19. Raz N, Gunning-Dixon F, Head D, Rodrigue K, Williamson A, Acker JD. **Regional volumetry of the cerebral cortex in normal adults: differential aging, sexual dimorphism, and hemispheric asymmetry.** *Neurobiol Aging*, in press
20. De Armond SJ, Fusco MM, Dewey MM. *Structure of the Human Brain: A Photographic Atlas.* New York: Oxford University Press, 1976
21. Duvernoy H. *The Human Brain: Surface, Three-dimensional Sectional Anatomy, and MRI*. Vienna: Springer, 1991
22. Shrout PE, Fleiss JL. **Intraclass correlations: uses in assessing raters reliability.** *Psychol Bull* 1990;86:420–428
23. Steiger JH. **Tests for comparing elements of a correlation matrix.** *Psychol Bull* 1980;87:245–251
24. Gunduz H, Wu H, Ashtari M, et al. **Basal ganglia volumes in first-episode schizophrenia and healthy comparison subjects.** *Biol Psychiatry* 2002;51:801–808
25. Giedd JN, Snell JW, Lange N, et al. **Quantitative magnetic resonance imaging of human brain development: ages 4–18.** *Cereb Cortex* 1996;6:551–560
26. Calabresi P, Centonze D, Bernardi G. **Cellular factors controlling neuronal vulnerability in the brain: a lesson from the striatum.** *Neurology* 2000;55:1249–1255
27. Volkow ND, Wang GJ, Fowler JS, et al. **Measuring age-related changes in dopamine D_2 receptors with ^{11}C-raclopride and ^{18}F-N-methylspiroperidol.** *Psychiatry Res* 1996;67:11–16
28. Bäckman L, Ginovart N, Dixon RA, et al. **Age-related cognitive deficits mediated by changes in the striatal dopamine system.** *Am Psychiatry* 2000;157:635–637
29. Kaasinena V, Rinne JO. **Functional imaging studies of dopamine system and cognition in normal aging and Parkinson's disease.** *Neurosci Biobehav Rev* 2002;26:785–793
30. Morris ED, Chefer SI, Lane MA, et al. **Loss of D_2 receptors binding with age in rhesus monkeys: importance of correction for differences in striatal size.** *J Cereb Blood Flow Metab* 1999;19:218–229
31. Rubin DC. **Frontal-striatal circuits in cognitive aging: evidence for caudate involvement.** *Aging Neuropsych Cog* 1999;6:241–259
32. Cho S, Jones D, Reddick WE, Ogg RJ, Steen RG. **Establishing norms for age-related changes in proton T1 of human brain tissue in vivo.** *Magn Reson Imaging* 1997;15:1133–1143
33. Blinkov SM, Glezer II. *The Human Brain in Figures and Tables*. New York: Basic Books, 1968
34. Gunter JL, Shiung MM, Manduca A, Jack CR. **Methodological considerations for measuring rates of brain atrophy.** *J Magn Reson Imaging,* 18:16–24.